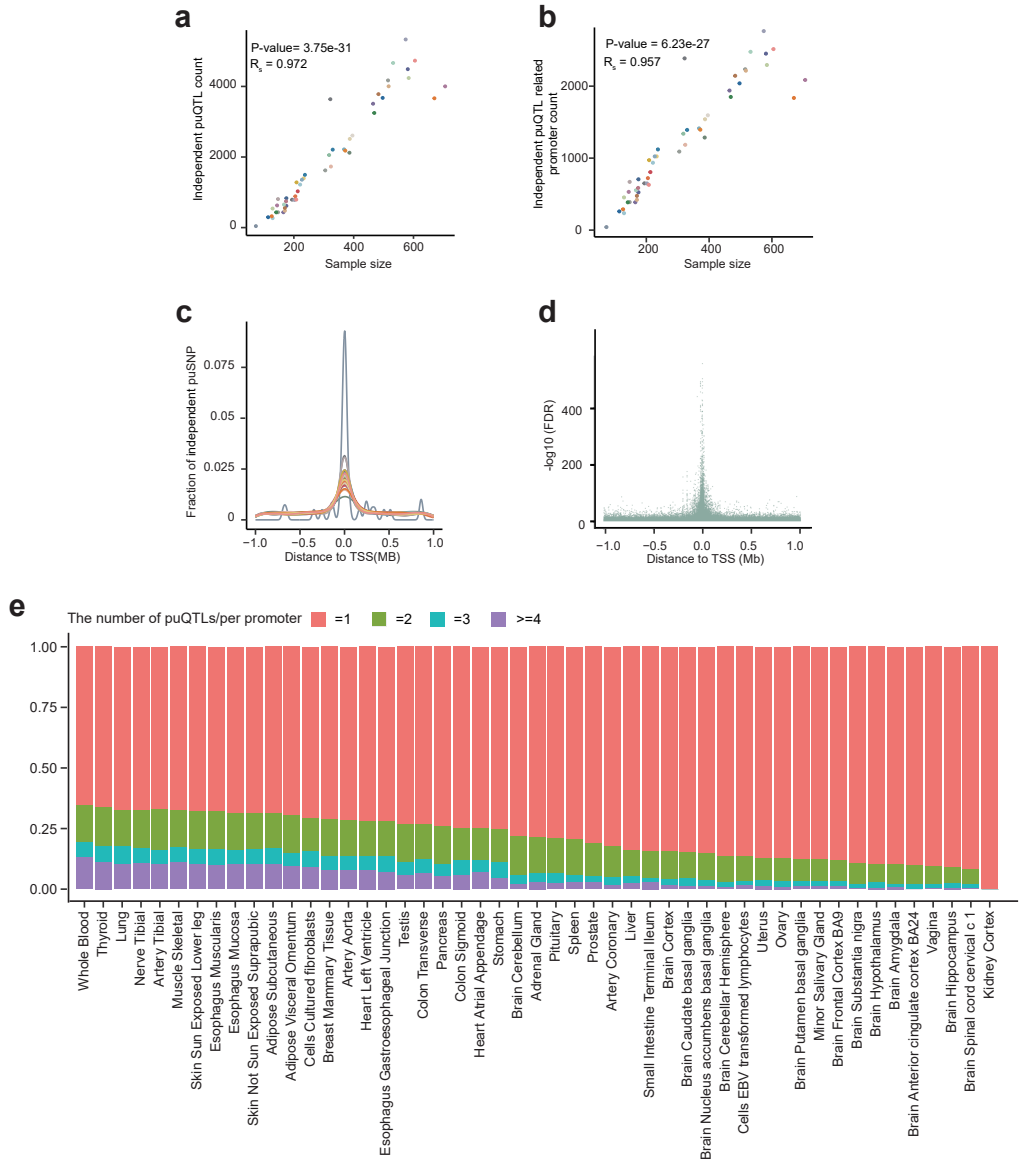

Supplementary Figure 1. A statistical summary of independent puQTLs in 49 tissues. (**a**) Correlation between the number of independent puQTL and sample size across 49 human tissues. The measure of correlation used is Spearman's correlation, and the corresponding *P*-value is reported. (**b**) Correlation between the number of independent puQTL associated promoters and sample size across 49 human tissues. (**c**) The distribution of the distance between independent puQTLs and their associated transcription start site (TSS) in 49 tissues. (**d**) The significance distribution of independent puQTLs around TSS. The FDR has been logarithmically transformed. (**e**) The proportion of independent puQTLs per promoter across the 49 human tissues, with different puQTL numbers per promoter depicted using four distinct colors.

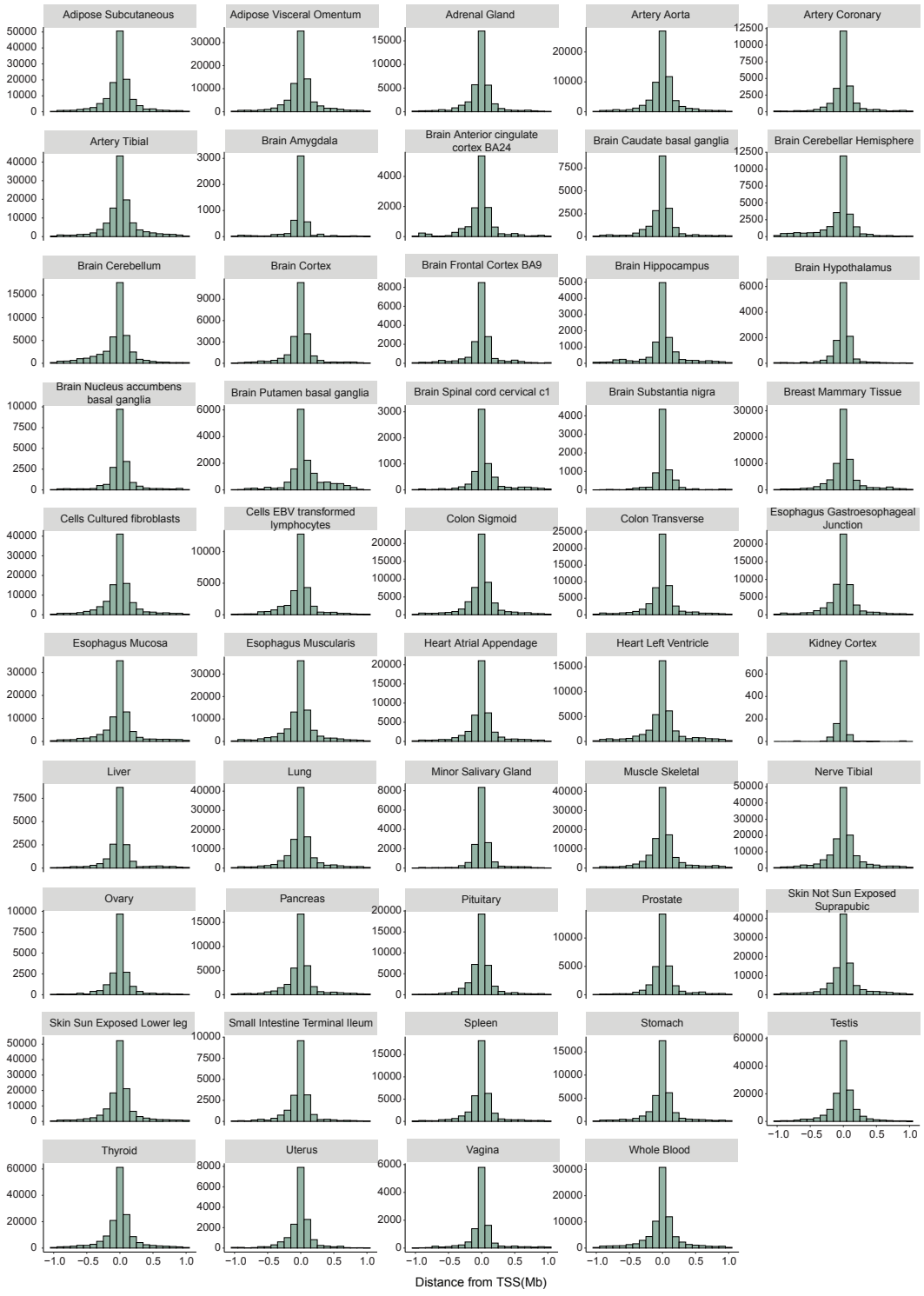

Supplementary Figure 2. An extensive examination of puQTLs in 49 tissues. The distribution of distances between puQTLs and their corresponding transcription start sites (TSS) within each tissue.

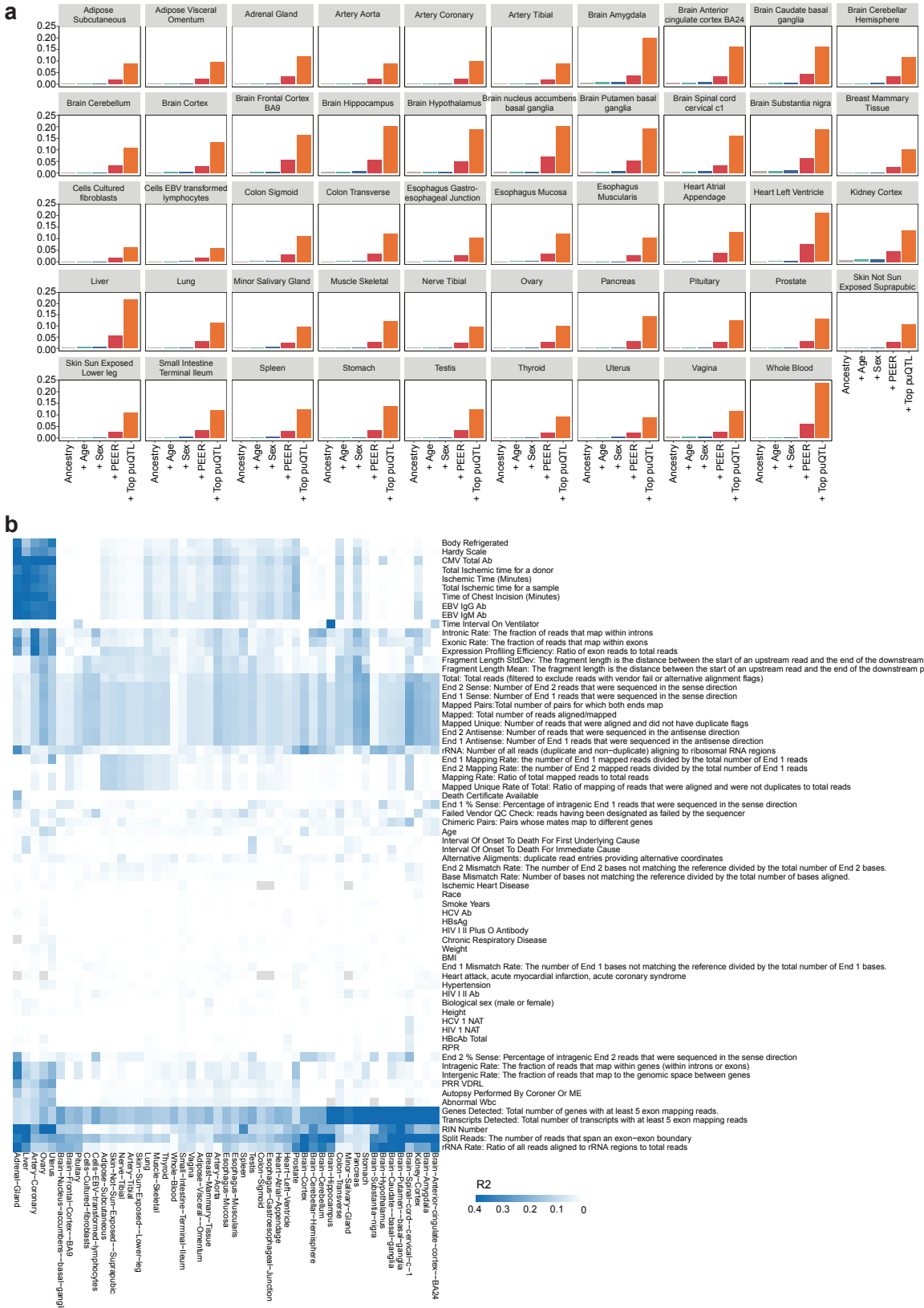
a
Adipose Subcutaneous
Adipose Visceral Omentum
Adrenal Gland
Artery Aorta
Artery Coronary
Artery Tibial
Brain Amygdala
Brain Anterior cingulate cortex BA24
Brain Caudate basal ganglia
Brain Cerebellar Hemisphere
Brain Cerebellum
Brain Cortex
Brain Frontal Cortex BA9
Brain Hippocampus
Brain Hypothalamus
Brain nucleus accumbens basal ganglia
Brain Putamen basal ganglia
Brain Spinal cord cervical c1
Brain Substantia nigra
Breast Mammary Tissue
Cells Cultured fibroblasts
Cells EBV transformed lymphocytes
Colon Sigmoid
Colon Transverse
Esophagus Gastro-esophageal Junction
Esophagus Mucosa
Esophagus Muscularis
Heart Atrial Appendage
Heart Left Ventricle
Kidney Cortex
Liver
Lung
Minor Salivary Gland
Muscle Skeletal
Nerve Tibial
Ovary
Pancreas
Pituitary
Prostate
Skin Not Sun Exposed Suprapubic
Skin Sun Exposed Lower leg
Small Intestine Terminal Ileum
Spleen
Stomach
Testis
Thyroid
Uterus
Vagina
Whole Blood
0.25
0.20
0.15
0.10
0.05
0.00
Ancestry
+ Age
+ Sex
+ PEER
+ Top puQTL
b
Body Refrigerated
Hardy Scale
CMV Total Ab
Total Ischemic time for a donor
Ischemic Time (Minutes)
Total Ischemic time for a sample
Time of Chest Incision (Minutes)
EBV IgG Ab
EBV IgM Ab
Time Interval On Ventilator
Intronic Rate: The fraction of reads that map within introns
Exonic Rate: The fraction of reads that map within exons
Expression Profiling Efficiency: Ratio of exon reads to total reads
Fragment Length StdDev: The fragment length is the distance between the start of an upstream read and the end of the downstream pair mate
Fragment Length Mean: The fragment length is the distance between the start of an upstream read and the end of the downstream pair mate
Total: Total reads (filtered to exclude reads with vendor fail or alternative alignment flags)
End 2 Sense: Number of End 2 reads that were sequenced in the sense direction
End 1 Sense: Number of End 1 reads that were sequenced in the sense direction
Mapped Pairs:Total number of pairs for which both ends map
Mapped: Total number of reads aligned/mapped
Mapped Unique: Number of reads that were aligned and did not have duplicate flags
End 2 Antisense: Number of reads that were sequenced in the antisense direction
End 1 Antisense: Number of End 1 reads that were sequenced in the antisense direction
rRNA: Number of all reads (duplicate and non−duplicate) aligning to ribosomal RNA regions
End 1 Mapping Rate: the number of End 1 mapped reads divided by the total number of End 1 reads
End 2 Mapping Rate: the number of End 2 mapped reads divided by the total number of End 1 reads
Mapping Rate: Ratio of total mapped reads to total reads
Mapped Unique Rate of Total: Ratio of mapping of reads that were aligned and were not duplicates to total reads
Death Certificate Available
End 1 % Sense: Percentage of intragenic End 1 reads that were sequenced in the sense direction
Failed Vendor QC Check: reads having been designated as failed by the sequencer
Chimeric Pairs: Pairs whose mates map to different genes
Age
Interval Of Onset To Death For First Underlying Cause
Interval Of Onset To Death For Immediate Cause
Alternative Aligments: duplicate read entries providing alternative coordinates
End 2 Mismatch Rate: The number of End 2 bases not matching the reference divided by the total number of End 2 bases.
Base Mismatch Rate: Number of bases not matching the reference divided by the total number of bases aligned.
Ischemic Heart Disease
Race
Smoke Years
HCV Ab
HBsAg
HIV I II Plus O Antibody
Chronic Respiratory Disease
Weight
BMI
End 1 Mismatch Rate: The number of End 1 bases not matching the reference divided by the total number of End 1 bases.
Heart attack, acute myocardial infarction, acute coronary syndrome
Hypertension
HIV I II Ab
Biological sex (male or female)
Height
HCV 1 NAT
HIV 1 NAT
HBcAb Total
RPR
End 2 % Sense: Percentage of intragenic End 2 reads that were sequenced in the sense direction
Intragenic Rate: The fraction of reads that map within genes (within introns or exons)
Intergenic Rate: The fraction of reads that map to the genomic space between genes
PRR VDRL
Autopsy Performed By Coroner Or ME
Abnormal Wbc
Genes Detected: Total number of genes with at least 5 exon mapping reads.
Transcripts Detected: Total number of transcripts with at least 5 exon mapping reads
RIN Number
Split Reads: The number of reads that span an exon−exon boundary
rRNA Rate: Ratio of all reads aligned to rRNA regions to total reads
R2
0.4
0.3
0.2
0.1
0
Adrenal−Gland
Liver
Artery−Coronary
Artery−Tibial
Uterus
Brain−Nucleus−accumbens−basal−ganglia
Brain−Frontal−Cortex−BA9
Prostate
Cells−Cultured−fibroblasts
Cells−EBV−transformed−lymphocytes
Adipose−Subcutaneous
Skin−Not−Sun−Exposed−Suprapubic
Kidney−Medulla
Artery−Tibial
Skin−Sun−Exposed−Lower−leg
Lung
Muscle−Skeletal
Whole−Blood
Thyroid
Small−Intestine−Terminal−Ileum
Vagina
Adipose−Visceral−Omentum
Breast−Mammary−Tissue
Artery−Aorta
Esophagus−Mucosa
Esophagus−Muscularis
Spleen
Testis
Colon−Sigmoid
Esophagus−Gastroesophageal−Junction
Prostate
Heart−Left−Ventricle
Heart−Atrial−Appendage
Brain−Cortex
Brain−Cerebellar−Hemisphere
Brain−Cerebellum
Brain−Hippocampus
Colon−Transverse
Minor−Salivary−Gland
Pancreas
Stomach
Brain−Substantia−nigra
Brain−Hypothalamus
Brain−Caudate−basal−ganglia
Brain−Putamen−basal−ganglia
Brain−Spinal−cord−cervical−c−1
Kidney−Cortex
Pituitary
Brain−Anterior−cingulate−cortex−BA24

Supplementary Figure 3. The optimization of a regression model for the identification of puQTLs. (**a**) Incorporation of various covariates, including ancestry principal components, age, sex, PEER factors, and the most strongly associated puQTLs. Specifically, the median value for all puQTL-associated genes across the 49 tissues is represented by the bars. (**b**) The association between inferred PEER factors and known technical, clinical and epidemiological covariates associated in each tissue.

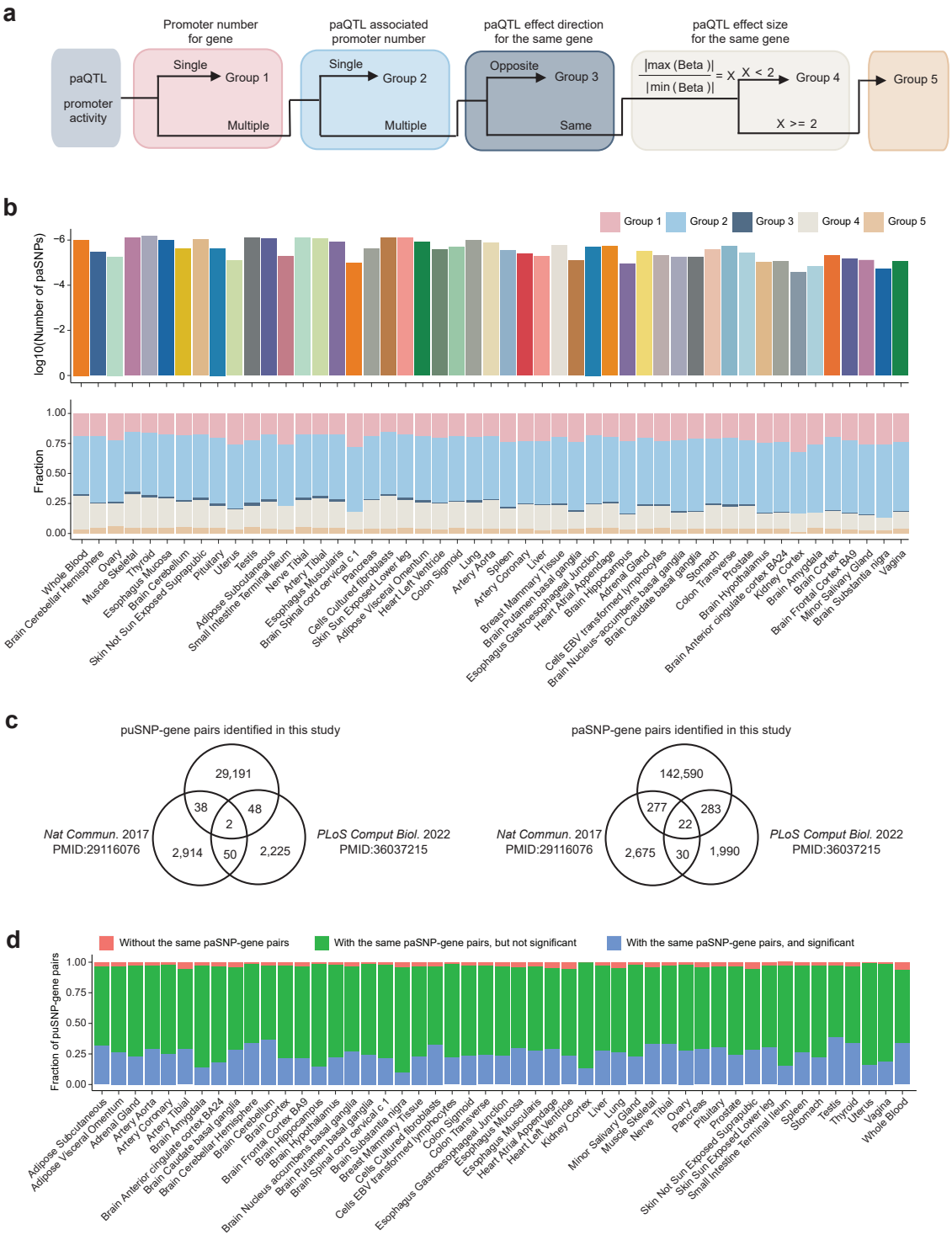

Supplementary Figure 4. Classification criteria and proportion of paQTL associated genes. (**a**) Classification procedure for the paQTL-associated genes. (**b**) The number of paSNPs in each tissue (top), and the fraction of paQTL associated genes within each group (bottom). The number

of paSNP is transformed by log10. (**c**) Overlapping between puSNP-gene pairs and paSNP-gene pairs identified in this study with CAGE based and RNA-seq-based paQTLs identified in previous publications. (**d**) The proportion of puQTLs did not mapped as paQTLs across 49 tissues. Red color represents puSNP-gene pairs that were not defined as paSNP-gene pairs; green color represents puSNP-gene pairs were defined as paSNP-gene pairs but not significant in paSNP-gene sets; blue color represents puSNP-gene pairs were also defined as signigicant paSNP-gene pairs.

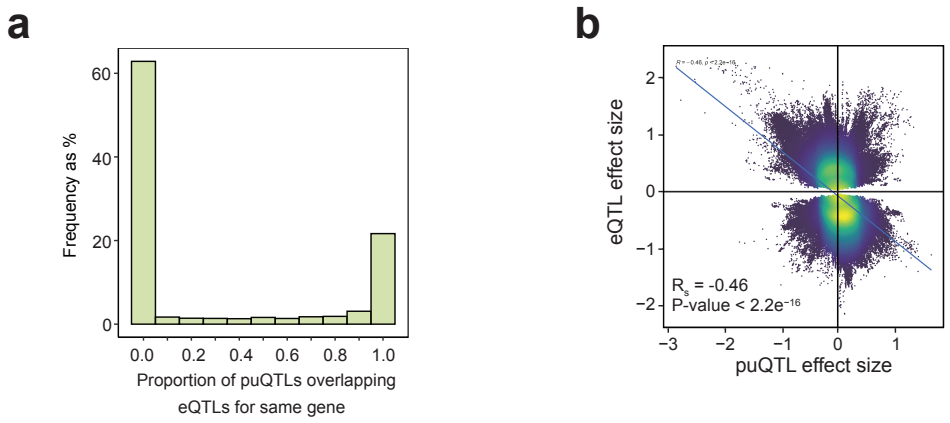

Supplementary Figure 5. Comparison between puQTLs and eQTLs. (**a**) The percentage of shared genetic variants associated with the same gene between puQTLs and eQTLs. The comparison accounts for puQTLs that share the same SNP ID as eQTLs, as well as puQTLs in high linkage disequilibrium (LD) with eQTLs ($r^2 \geq 0.6$). The analysis focuses on genetic variants that are jointly associated with the same gene by both puQTLs and eQTLs. (**b**) Overall correlation between the effect size of puQTLs and eQTLs. The measure of correlation used is Spearman's correlation, and the corresponding *P*-value is reported.

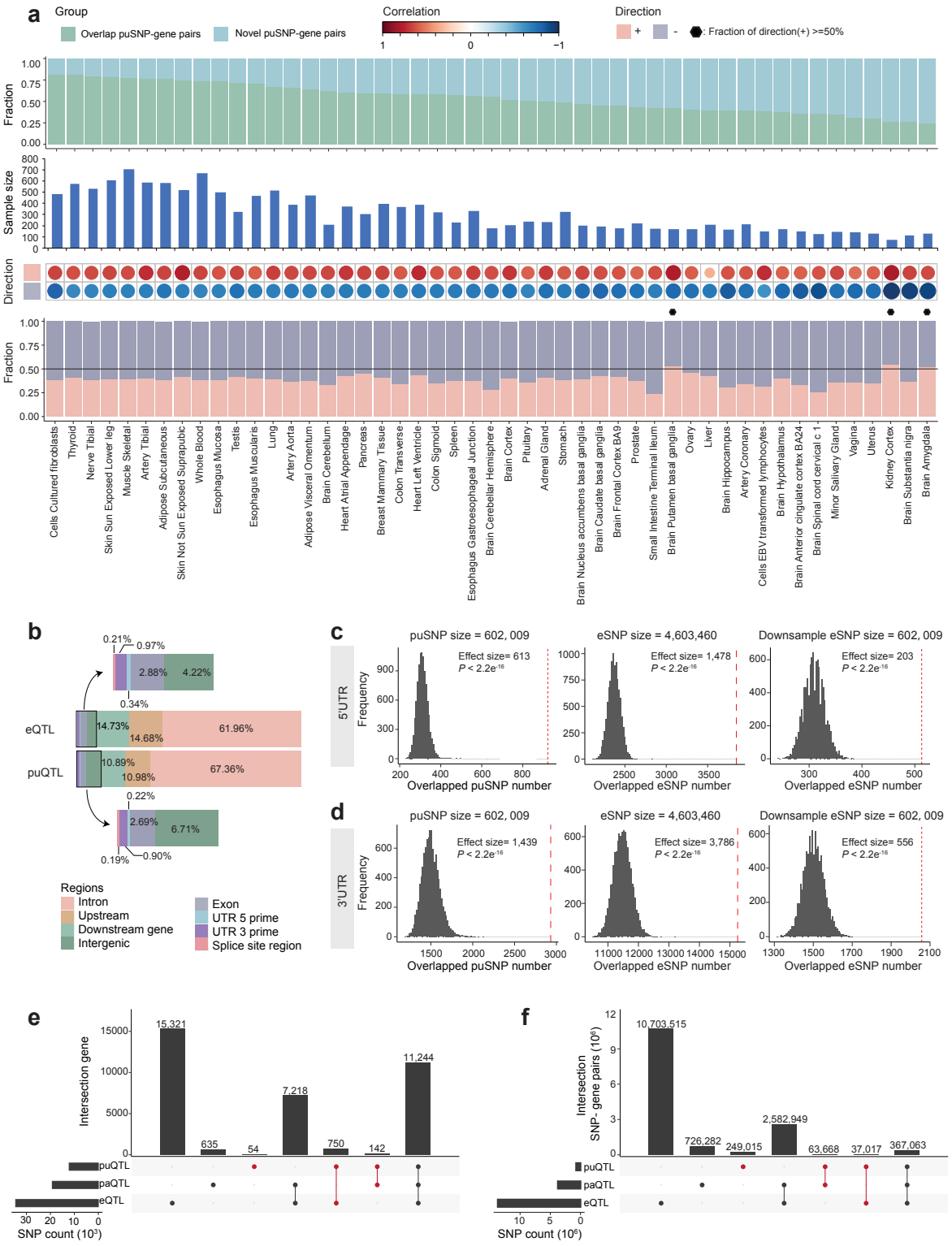

Supplementary Figure 6. Comparative analysis of genomic features in puQTLs and eQTLs.

(**a**) Investigation of gene overlap and correlation in puGenes and eGenes across different tissues.

In the top panel, the overlap between puGenes and eGenes for each tissue. The puGenes that overlap with eGenes are depicted in green, while non-overlapping genes are considered novel puGenes and are shown in blue. The graph below shows the sample size in a matched order. For the genes that overlap between puGenes and eGenes, the positive and negative correlation coefficients are shown a circle plot in the middle panel. The size and color of the circles represent the correlation value. In the bottom panel, the fraction of puGenes that positively or negatively correlate with eGenes in each tissue. puGenes with a positive correlation are depicted in pink, while those with a negative correlation are shown in grey. These tissues where more than 50% of the overlapped puGenes have a positive correlation with eGenes were marked with an asterisk (*) at the top of the chart. (**b**) Comparative analysis of eQTLs and puQTLs in different functional categories. The proportion of eQTLs (top) and puQTLs (bottom) within various functional categories as defined by SnpEff v.5.0. (**c**) Enrichment analysis of puSNPs, eSNPs, and downsampled eSNPs in the 3'UTR. The red line represents the observed overlap number of these SNPs in the 5'UTR. The histograms demonstrate the expected overlap between puSNPs, eSNPs, and downsampled eSNPs based on randomly shuffled peaks from 10,000 simulations. Significant differences between the expected and observed values are indicated, and *P*-values were generated by empirical test. The same parameters are applied to the histograms presented below. (**d**) Enrichment analysis of puSNPs, eSNPs, and downsampled eSNPs in the 5'UTR. (**e**) Overlap of genes associated with puQTLs, paQTLs and eQTLs. The overlapping gene set specifically related to puQTLs is highlighted in red. (**f**) Overlap of puSNP-gene pairs, paSNP-gene pairs and eSNP-gene pairs. The overlapping set specifically related to puSNP-gene pairs is highlighted in red.

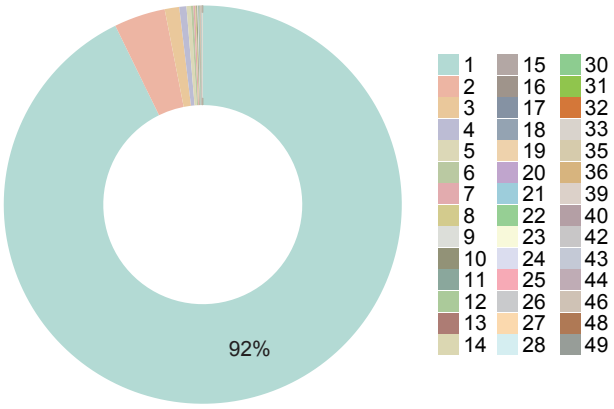

Supplementary Figure 7. The tissue specificity of independent puQTLs. The circle plot visualizing the number of independent puQTLs shared across different tissues, with each color representing a specific number of shared tissues.

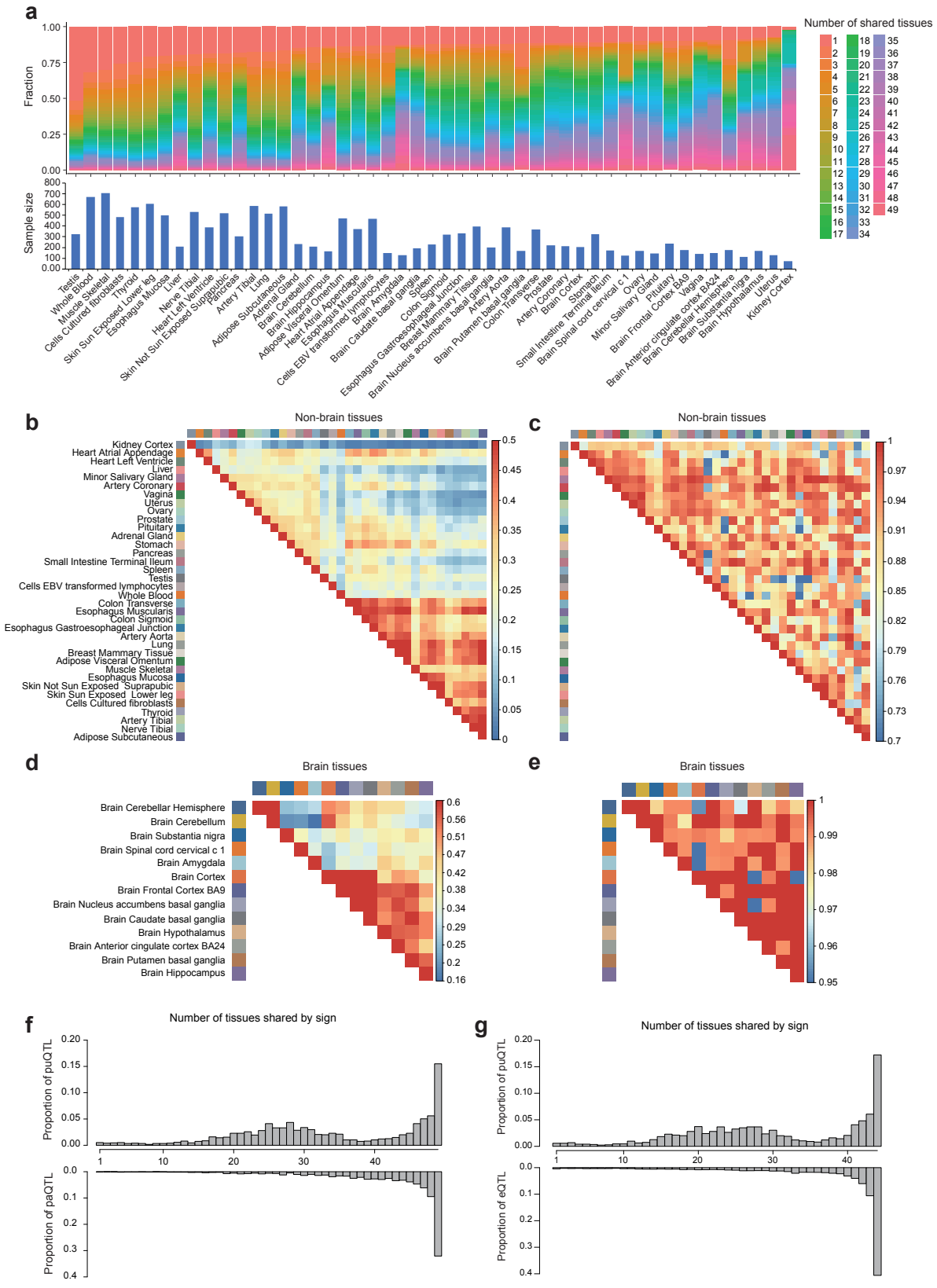
a
Fraction
Sample size
Number of shared tissues
Testis
Whole Blood
Muscle Skeletal
Cells Cultured fibroblasts
Thyroid
Skin Sun Exposed Lower leg
Esophagus Mucosa
Liver
Nerve Tibial
Heart Left Ventricle
Skin Not Sun Exposed Suprapubic
Pancreas
Artery Tibial
Lung
Adipose Subcutaneous
Adrenal Gland
Brain Cerebellum
Adipose Visceral Omentum
Brain Hippocampus
Heart Atrial Appendage
Esophagus Muscularis
Cells EBV transformed lymphocytes
Brain Amygdala
Brain Caudate basal ganglia
Spleen
Colon Sigmoid
Esophagus Gastroesophageal Junction
Breast Mammary Tissue
Brain Nucleus accumbens basal ganglia
Artery Aorta
Brain Putamen basal ganglia
Colon Transverse
Prostate
Artery Coronary
Brain Cortex
Stomach
Small Intestine Terminal Ileum
Brain Spinal cord cervical c 1
Ovary
Minor Salivary Gland
Pituitary
Vagina
Brain Frontal Cortex BA9
Brain Anterior cingulate cortex BA24
Brain Cerebellar Hemisphere
Brain Substantia nigra
Brain Hypothalamus
Uterus
Kidney Cortex
b
Non-brain tissues
c
Non-brain tissues
d
Brain tissues
e
Brain tissues
f
Number of tissues shared by sign
Proportion of puQTL
Proportion of paQTL
g
Number of tissues shared by sign
Proportion of puQTL
Proportion of eQTL

Supplementary Figure 8. Specificity of puQTLs in brain and non-brain tissues. (**a**) Proportion of shared puQTLs across various tissues. The number of shared tissues is indicated using a color code for puQTLs in each specific tissue. The graph below shows the sample size in a matched order. (**b**) Pairwise sharing of puQTLs by magnitude among non-brain tissues. (**c**) Pairwise sharing of puQTLs by sign among non-brain tissues. (**d**) Sharing of puQTLs by magnitude among brain tissues. (**e**) Pairwise sharing of puQTLs by sign among brain tissues. (**f**) Histograms showing the fraction of puQTLs (top) and paQTLs (bottom) shared across different number of tissues by sign. (**g**) Histograms showing the fraction of puQTLs (top) and eQTLs (bottom) shared across different number of tissues by sign.

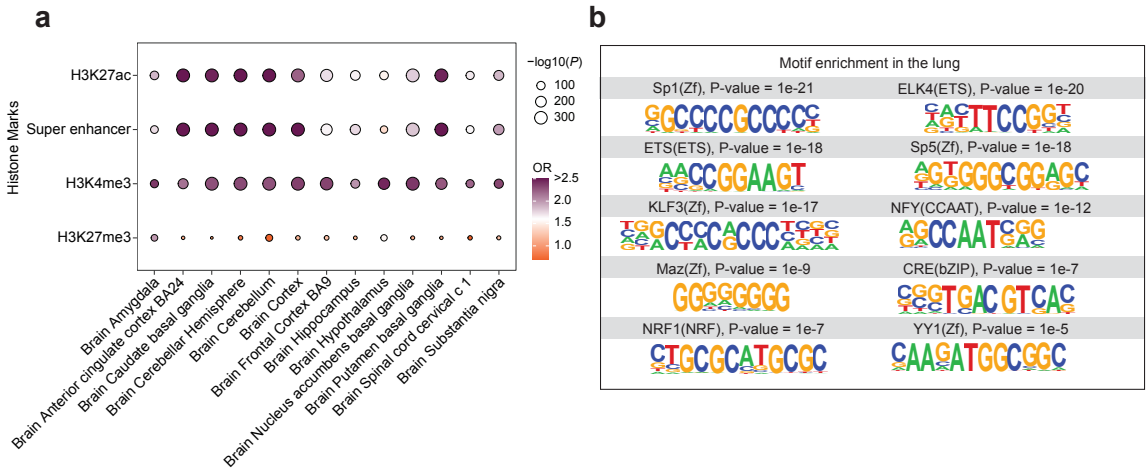

Supplementary Figure 9. The enrichment of puQTLs within epigenetic marker binding regions. (**a**) Significant enrichment of puQTLs within different histone markers occupied regions. The odds ratio is represented by the color of each dot, while the *P*-value (logarithmically transformed) is indicated by the dot size. (**b**) Motif enrichment in the lung.

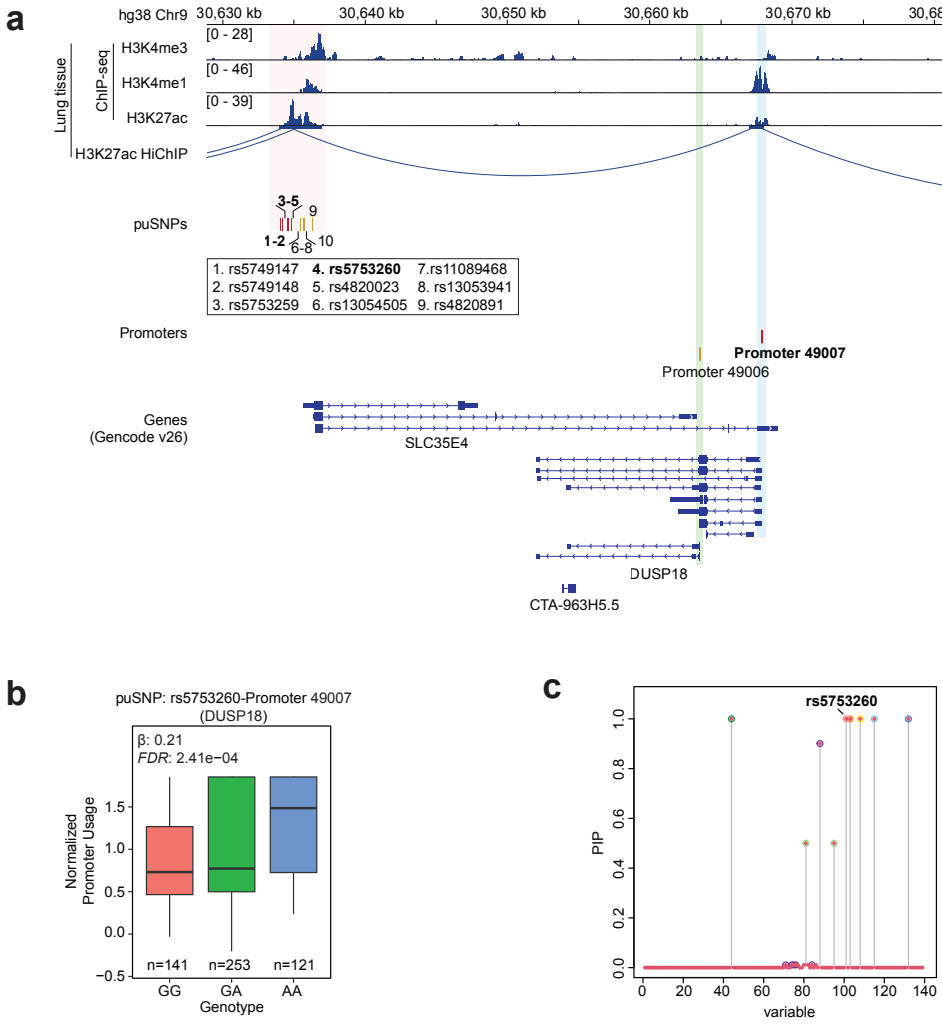

Supplementary Figure 10. The associations between the presence of puSNP rs5753260 and the usage of promoter 49007 in *DUSP18* gene. (**a**) Integrated genome view of the lead puSNP rs2240002 and five LD puSNPs (rs5749147, rs5749148, rs5753259, rs5753260, rs4820023) and their adjacent regions, displaying H3K27ac HiChIP loops and ChIP-seq of epigenetic markers in lung tissue. (**b**) The associations between the genotypes of LD puSNP rs5753260 and the promoter usage of promoter 49007 in gene *DUSP18* in lung tissue. The center line represents the median with the box spanning the 25th to 75th percentiles. The whiskers extend to values within 1.5 times the interquartile range (IQR) from the box's ends. n represents the sample size for the corresponding genotypes. (**c**) Fine-mapping analysis indicated that LD puSNP rs5753260 function as causal SNPs in regulating the usage of promoter 49007 in the *DUSP18* gene.

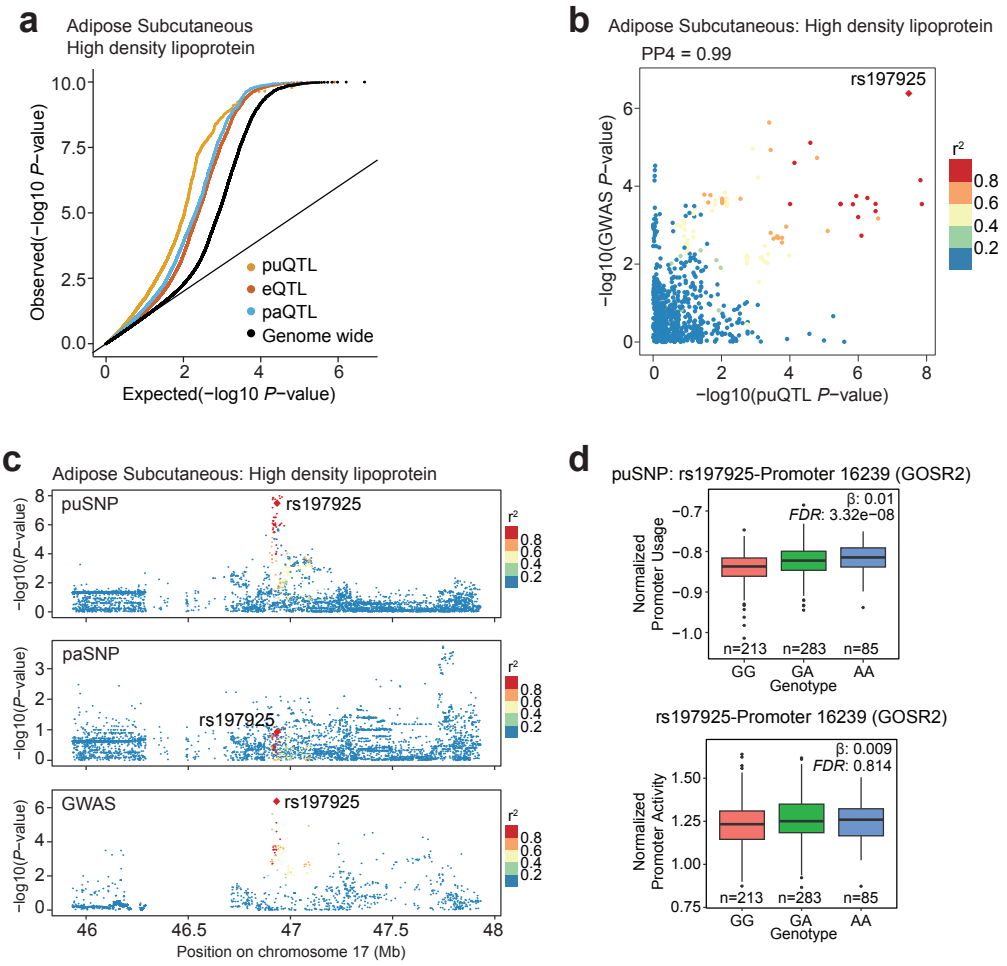

Supplementary Figure 11. Colocalization results between puQTL rs197925 and trait associated GWAS signals in adipose subcutaneous. (**a**) A quantile–quantile (Q-Q) plot of high density lipoprotein GWAS *P*-values compares puQTLs, paQTLs, and eQTLs with genome-wide SNPs in the adipose subcutaneous. The y-axis represents the observed GWAS P-values from association test, while the x-axis shows the expected *P*-values under the null hypothesis of no association (two-sided). (**b**) Colocalization of puQTLs with high density lipoprotein GWAS signals in the adipose subcutaneous, with posterior probability (PP4) estimated by Bayesian colocalization analysis. The x-axis and y-axis represent *P*-values from association tests for puQTL and GWAS, respectively (two-sided). (**c**) The LocusZoom plot depicts a 1 Mb region centered around the lead SNP rs197925. The y-axis represents *P*-values from association tests between SNPs and *GOSR2* promoter usage (top), promoter activity (middle) and high density lipoprotein (bottom) in the adipose subcutaneous (two-sided). SNPs represented by the dots are colored based on their LD (r^2) with rs197925. (**d**) The boxplots showing the effect size and significance of rs197925 on the promoter usage (top) and promoter activity (bottom) of promoter 16239 in the

adipose subcutaneous. The center line represents the median with the box spanning the 25th to 75th percentiles. The whiskers extend to values within 1.5 times the interquartile range (IQR) from the box's ends. n represents the sample size for the corresponding genotypes.

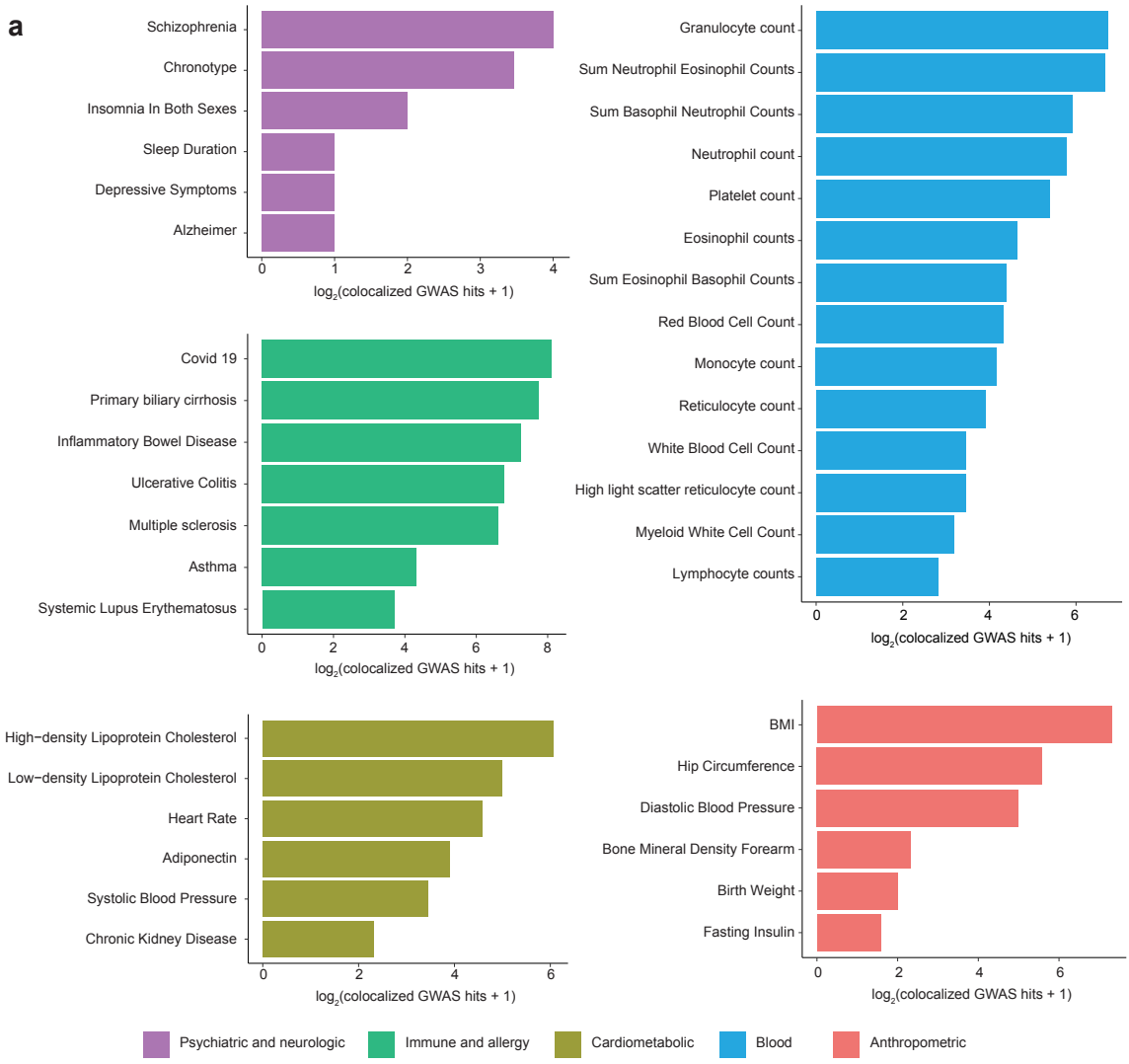

Supplementary Figure 12. Colocalization results between puQTLs and trait associated GWAS signals. (**a**) The number of puQTL-colocalized with GWAS hits for each GWAS trait

stratified by GWAS trait category and colocalization group. (**b**) The number of puQTL-colocalized GWAS hits in different tissues, represented on the y-axis.

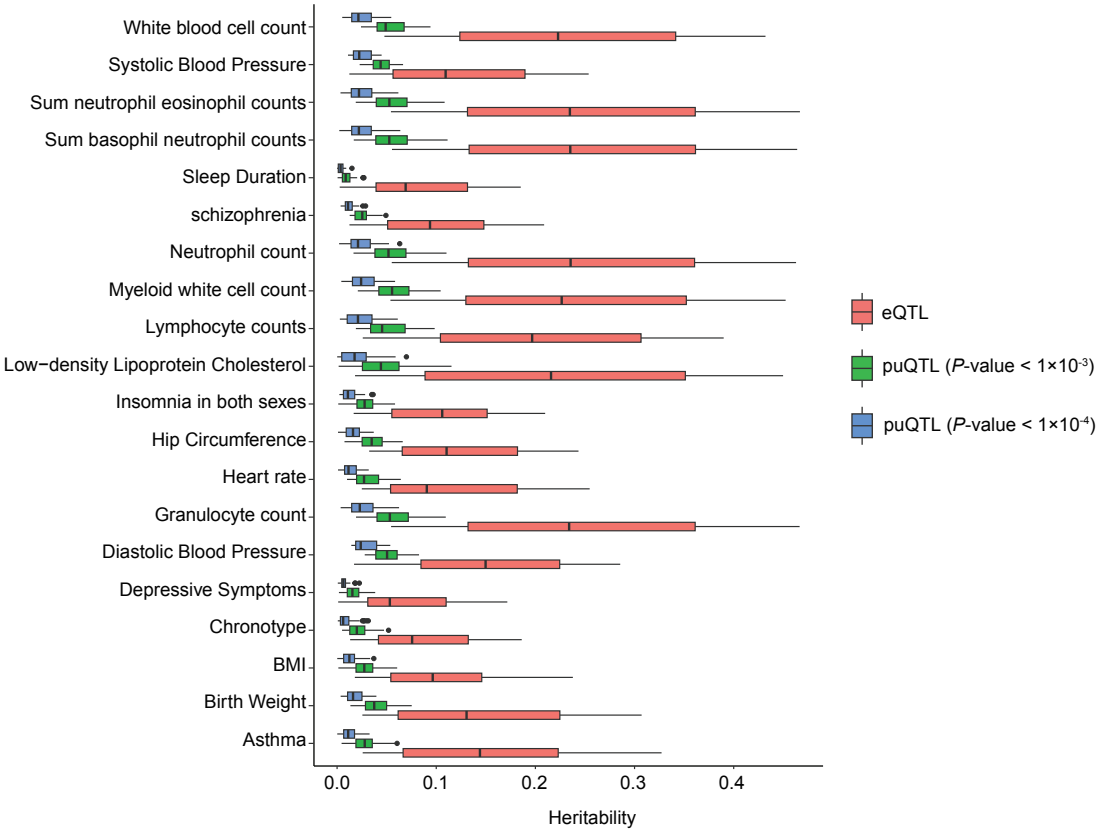

Supplementary Figure 13. The proportion of heritability explained by eQTLs and puQTLs across 49 tissues for 20 GWAS traits. The puQTLs are chosen using two thresholds: *P*-value < 10^{-3} and 10^{-4}. The box plot visualizes the central tendency, with the median values shown as the center line, and the interquartile range (25^{th} to 75^{th} percentile) depicted as the box.

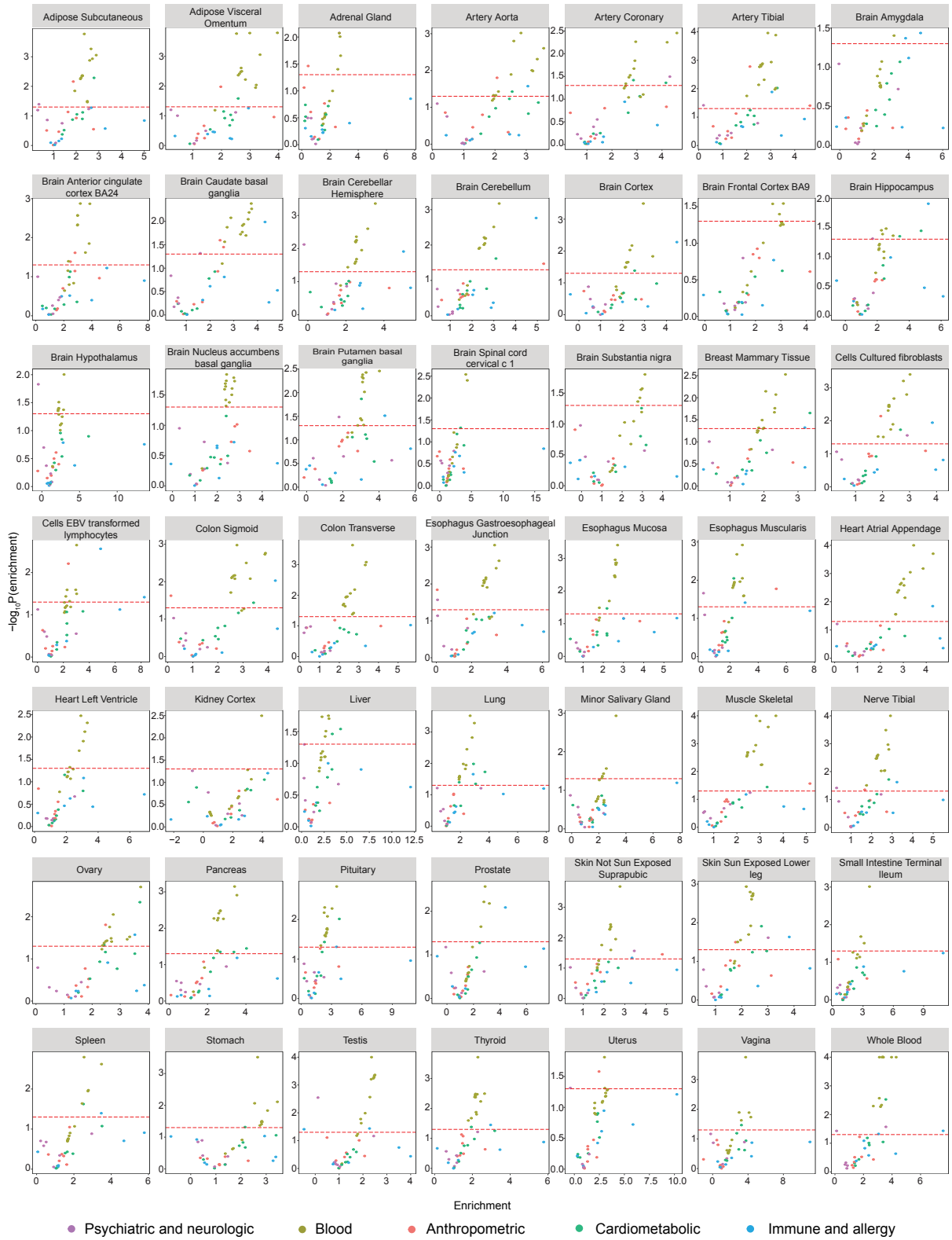

Supplementary Figure 14. The heritability enrichment of 40 GWAS traits across 49 tissues.

The heritability enrichment analysis of 40 GWAS traits was divided into five categories: anthropometric, cardiometabolic, psychiatric and neurologic, blood, immune and allergy. To assess the heritability enrichment, puQTLs were used with a threshold of 10^{-3}. The significance threshold, represented by a dashed line, was set at a *P*-value of 0.05, with different color representing different categories of trait.

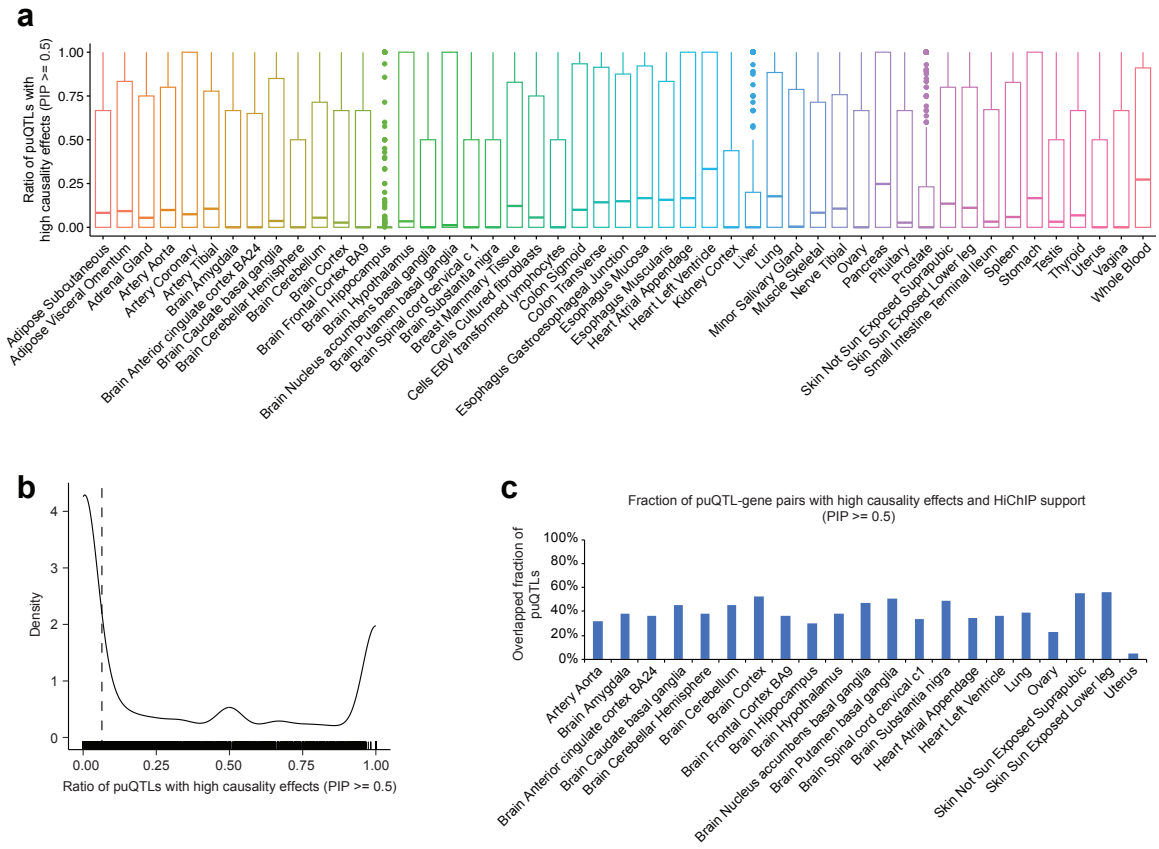

Supplementary Figure 15. The fine-mapping results for puQTLs across 49 tissues. (**a**) The ratio of puQTLs showing high causality effect (PIP>=0.5) across 49 tissues, with different color representing different tissue. The center line represents the median with the box spanning the 25th to 75th percentiles. The whiskers extend to values within 1.5 times the interquartile range (IQR) from the box's ends. (**b**) The density distribution of the aforementioned ratio of puQTLs manifesting high causality effects. Notably, the median causality ratio for puQTLs is quantified at 0.07. (**c**) Fraction of puQTL-gene pairs with both high causality effects and HiChIP data support.